Cone Penetration Testing 2018 – Hicks, Pisanò & Peuchen (Eds)

Realistic numerical simulations of cone penetration with advanced soil models

Zhandos Y. Orazalin
Singapore-MIT Alliance for Research and Technology, Singapore

Andrew J. Whittle
Massachusetts Institute of Technology, Cambridge, MA, USA

ABSTRACT: The analysis of soil penetration represents a challenging class of geotechnical problems due to large deformations, high gradients of the field variables (stresses, strains, pore pressures, etc.) around the penetrometer, the various drainage conditions and complex constitutive behavior of soils. Most prior research using large deformation Finite Element (FE) methods has been limited to simplified assumptions on drainage conditions and constitutive behavior. Following earlier work by Hu & Randolph (1998), we propose a finite element analysis procedure using automated remeshing and solution mapping within a commercial FE solver (ABAQUS Standard) in order to simulate quasi-static piezocone penetration using advanced effective stress soil models. Predictions of piezocone penetration using the proposed FE analyses are evaluated through comparison with undrained *steady state* analytical solutions obtained from the Strain Path Method and with field measurements from Boston. Predictions of partially drained penetration are compared with recently published 2-phase MPM analyses and with data from laboratory (1g and centrifuge) model tests in kaolin.

1 INTRODUCTION

Piezocone testing is widely used in geotechnical engineering to investigate subsurface stratigraphy and to estimate engineering properties of pertinent soil units based (primarily) on measurements of tip resistance and penetration pore pressures. Most quantitative interpretations of the data are based on empirical classification schemes and correlations. The theoretical basis for estimating parameters such as undrained shear strength in homogenous, low permeability clays is also well established using the Strain Path Method (SPM; Baligh, 1985; Teh & Houlsby, 1991) in conjunction with relevant constitutive models. However, there is clearly a need for more comprehensive predictive capabilities for interpreting penetration in soils of transitional permeability and in interpreting piezocone signatures in layered soil systems.

Finite element analyses offer a general framework for tackling these large deformation problems. Special procedures are needed to control mesh distortions when using conventional Lagrangian FEM, (e.g., RITSS; Hu & Randolph, 1998) while more advanced methods (ALE: van den Berg, 1984; MPM: Beuth et al., 2012) mitigate this problem by considering the Eulerian flow of soil particles through a mesh. Nearly all of the published studies for cone penetration use total stress analyses and highly simplified models of soil behavior (e.g., linearly elastic perfectly-plastic, EPP). Only two studies have specifically considered partial drained piezocone penetration: 1) Yi et al. (2012) use a conventional updated Lagrangian formulation for coupled consolidation (ABAQUS/Standard; with local controls on mesh distortion) together with an EPP model; while 2) Ceccato et al. (2016) use a two-phase mixture MPM program (Anura3D, 2017) with the Modified Cam Clay soil model (MCC; Roscoe & Burland, 1968).

This paper proposes a numerical procedure for simulating large deformation piezocone penetration using an *automated* mesh-to-mesh solution mapping procedure in Abaqus/Standard™ (Simulia, 2016) which is conceptually similar to RITSS (Remeshing and Interpolation Technique with Small Strain). This method enables simulation of partially-drained coupled consolidation with advanced effective stress soil models.

2 METHODOLOGY

Figure 1 illustrates the general algorithm proposed for finite element analyses of cone penetration. The procedure combines conventional Lagrang-

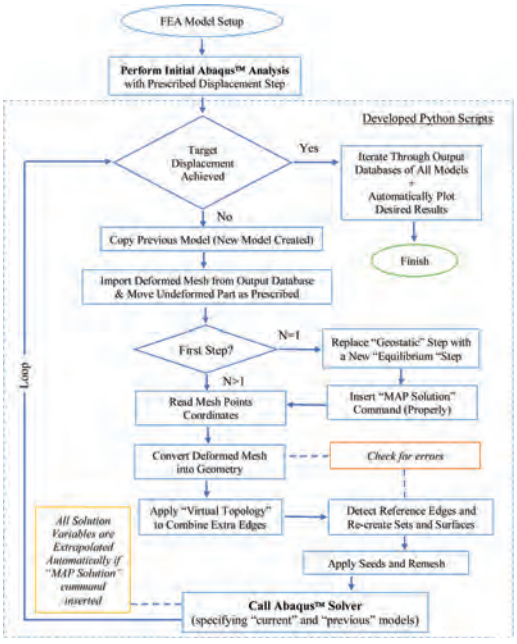

Figure 1. General algorithm for automated re-meshing and solution mapping in FE analysis (Orazalin, 2017).

ian FEM with separate remeshing (of the entire domain) and solution mapping and interpolation of the solution variables (stresses, pore pressures, state variables, etc.), using the mesh-to-mesh feature available in Abaqus/Standard.

This is controlled through a scripting interface (that uses the same syntax and operators as Python) that allows users to bypass Abaqus Environment's Graphical User Interface and communicate directly with the program kernel. After each remeshing step, a single Command is needed to initiate creation of the new FE model:

mdb.Model(name = *newmodel*, objectToCopy = mdb.models[*oldmodel*])

The accuracy of the analysis depends on the success of the interpolation employed to map the solution variables. This is especially important for complex models with (discontinuous) history-dependent state variables. The only required input is the frequency of remeshing which can be tailored to the specific problem of interest.

Figure 2a shows the geometry of the FE model for simulating axisymmetric cone penetration. Coupled consolidation within the soil mass is represented using 4-noded triangular elements (CAX4P) with bilinear interpolation of displacements and pore pressures and full integration of element stresses. The model uses an unstructured mesh constructed using an advancing front method-Delaunay algorithm (Borouchaki et al., 2000). The penetrometer is specified as a rigid shell with a rounded tip geometry (Fig. 2b) which approximates the simple pile geometry (Baligh, 1985). Previous studies (Aubeny, 1992) have found this to be a good approximation for the standard 60° conical tip while mitigating potential numerical problems associated with singular stress points.

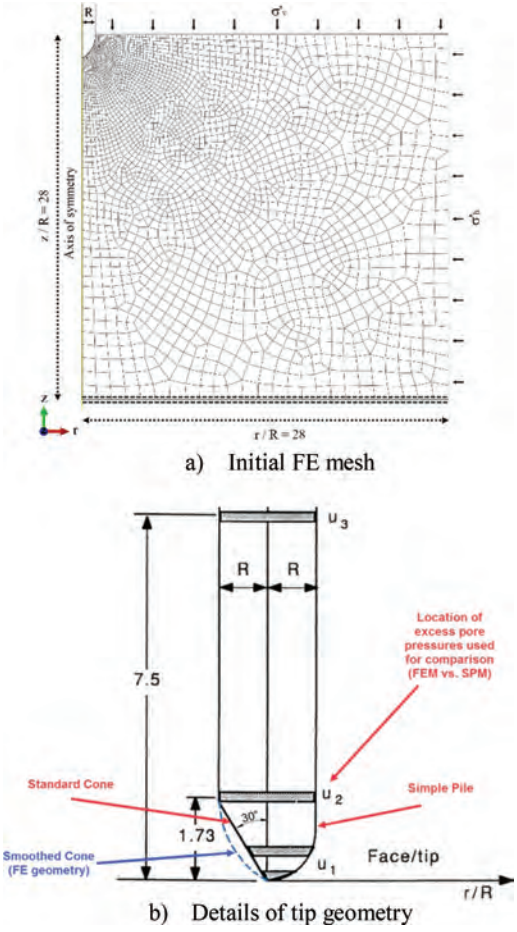

Figure 2. Finite element model of axisymmetric piezocone penetration.

Contact between the penetrometer and soil is tracked using a finite sliding formulation (Simulia, 2016) which requires that the master surface (penetrometer) has a continuous surface normal at all points in order to avoid numerical convergence problems. Abaqus automatically smooths the transition between element facets along the master surface using a control parameter, f:

$f = \alpha_1/l_1 = \alpha_2/l_2$

where l_1 and l_2 are the lengths of the adjacent facets and α_1, α_2 the associated transition lengths.

In order to maintain accuracy in tracking the contact surface through multiple cycles of re-meshing and interpolation, the analyses use f = 0.01, with re-meshing conducted at fixed penetration intervals, $\Delta y/R = 0.1$. The current analyses assume smooth, frictionless contact between the penetrometer and the soil ($\delta = 0°$).

The FE model represents a standard piezocone (R = 1.78cm) moving vertically at specified displacement rate, v, within a homogenous element of soil (0.5m high with radius 0.5m; i.e., z/R = 28 = r/R). The model simulates a calibration chamber configuration (i.e., uniform initial stress state) with an initial vertical effective stress, $\sigma'_{v0} = 100$kPa applied as a surcharge at the top surface and K_0 conditions (controlled by stress history). The far boundaries (lateral and base) are free draining (zero excess pore pressures), while the top surface is assumed to be impermeable. The current analyses assume that the tip of the penetrometer is embedded within the clay (i.e., there is a perturbation of the initial stress field to achieve drained equilibrium), in order to simplify the computations.

The proposed procedure has proved to provide a robust framework that can be used in conjunction with a range of advanced effective stress models of soil behavior. Here, we compare predictions for two rate independent elasto-plastic models, Modified Cam Clay (MCC; Roscoe & Burland, 1968) and MIT-E3 (Whittle & Kavvadas, 1994) using parameters corresponding to resedimented BBC (Boston Blue Clay). The MIT-E3 model is able to describe aspects of the non-linear and anisotropic stress-strain-strength properties measured in laboratory element tests (Whittle et al., 1994). All of the analyses assume a constant hydraulic conductivity, $k = 1 \times 10^{-7}$ cm/s. The two soil models are integrated within Finite Element solvers through UMAT (user-defined material model) subroutines (Hashash, 1992; Akl, 2010; Orazalin, 2015) and have been compared in prior analyses of penetrometer tests in clays using the Strain Path Method (Aubeny, 1992; Aubeny & Whittle, 1992).

3 UNDRAINED PENETRATION

Figure 3 shows the remeshing process and typical predictions of the excess pore pressures at several different tip depths. The results in Figure 4 compares finite element predictions for standard piezocone penetration (v = 2cm/s) in K0-consolidated BBC using the MCC and MIT-E3 soil models. Automatic remeshing (and interpolation) has been carried out at fixed intervals in these analyses ($\Delta z/R = 0.1$), such that there is no apparent distortion in the meshes shown in Figure 3, while effects

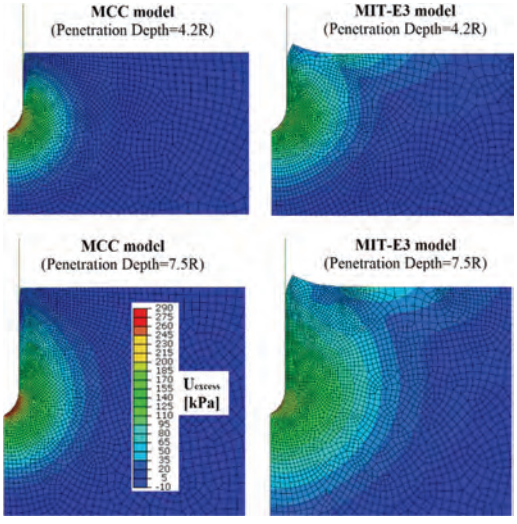

Figure 3. Excess pore pressure fields for undrained penetration in K_0-normally consolidated BBC (MCC and MIT-E3 models).

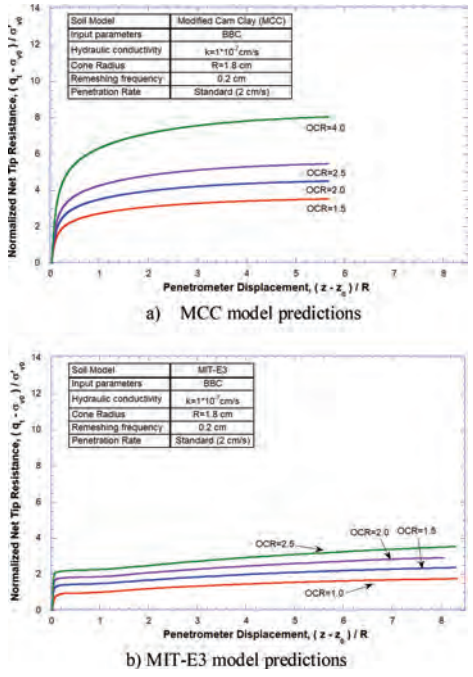

Figure 4. Effect of soil model and stress history on predictions of undrained penetration resistance.

of the initial embedment are seen in the excess pore pressures near to the top surface. There is minimal migration of pore water within the model (this is readily checked by increasing the displacement

rate). The computed excess pore pressures around the tip of the penetrometer at z/R = 5.5 are in close agreement with prior Strain Path analyses using the same soil models (Aubeny, 1992).

Figure 4a shows the computed net tip resistance, $(q_t-\sigma_{v0})/\sigma'_{v0}$ as a function of the penetration depth for the MCC soil model with OCR's ranging from 1.0–4.0. These results show rapid convergence towards steady state penetration conditions. In contrast, predictions for MIT-E3 (Fig. 4b) show the tip resistance increasing more gradually with penetration depth. This result can be attributed to the effects of non-linear shear stiffness at small strains, that generate a much larger zone of excess pore pressures around the penetrometer. The current analyses were extended to a total depth, z/R = 8.25, at which point the excess pore pressures were affected by proximity to the base boundary in the model.

Figure 5a compares the net tip resistance from the current finite element and prior steady state Strain Path analyses (presented by Aubeny, 1992).

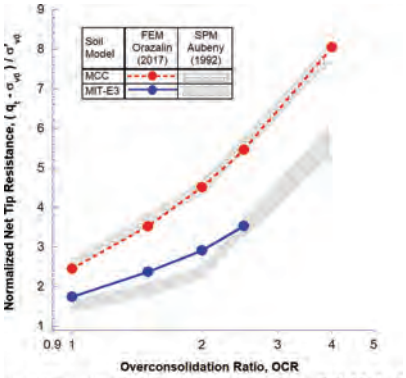

a) Comparison with predictions from Strain Path Method (Aubeny, 1992)

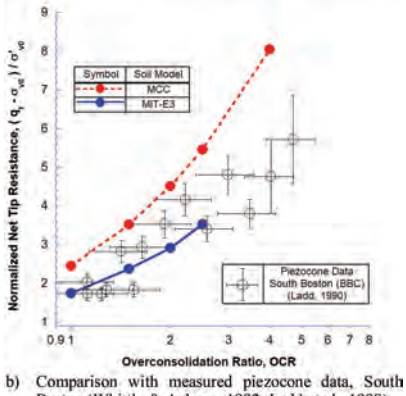

b) Comparison with measured piezocone data, South Boston (Whittle & Aubeny, 1992; Ladd et al., 1998)

Figure 5. Evaluation of FE predictions of undrained penetration resistance in BBC.

There is excellent agreement between the two sets of analyses for MCC (for OCR = 1.0–4.0). The FE predictions for MIT-E3 (interpreted at the final penetration depth) are also in reasonable agreement with the prior SPM analyses but further refinements are needed to establish steady state conditions in the FE model.

Differences in the computed tip resistance from the two soil models can be linked to the undrained strength anisotropy of MIT-E3. The two models exhibit similar shear strength in triaxial compression, but MIT-E3 predicts lower strength in the direct simple shear and extension models (s_{uDSS}/s_{uTC} = 0.65, s_{uTE}/s_{uTC} = 0.64, respectively, at OCR = 1.0).

There are several well documented sets of piezocone data in BBC. Figure 5b compares results from tests published by Ladd et al. (1998) from the CA/T Special Test Site in South Boston. The results show the mean and standard deviation of the net cone resistance and OCR computed over 3m (10ft) intervals through the full depth (43+m) of the clay. The data show significant scatter in net tip resistance with OCR. However, it is apparent that the MCC model generally overestimates the measured behavior, while MIT-E3 is in better agreement with the data (especially at low OCR).

4 EFFECTS OF PARTAL DRAINAGE

Partial drainage refers to the situation where there is concurrent generation and dissipation of excess pore pressures during steady penetration. McNeilan and Bugno (1984) showed that resistance (of a standard 10cm^2 cone at 2cm/s) was closely correlated with the hydraulic conductivity of silts at four sites where k ranged from 10^{-7}–10^{-4} cm/s. The reported tip resistance for drained penetration (k > 10^{-4}cm/s) were a factor of 7 larger than that measured in undrained situations (k ≤ 10^{-7}cm/s). Suzuki and Lehane (2014) investigated partial drainage in lightly overconsolidated Burswood clay by varying the penetration rates in the range v = 2 × 10^{-5}–2.0cm/s. Their data showed a factor of 2 difference between drained and undrained penetration. The highest tip resistance at the slowest penetration rate (fully drained) but the lowest tip resistance occurred in the range 0.02–0.2cm/s suggesting that penetration properties are also influenced by rate-dependent soil behavior.

Partial drainage effects can be readily simulated in the proposed FE analyses by varying either the penetration rate, hydraulic conductivity or size of the cone. Results in Figure 6 show typical predictions of penetration tip resistance (in the calibration chamber model, Fig. 1) using the MCC soil model for normally consolidated BBC at penetra-

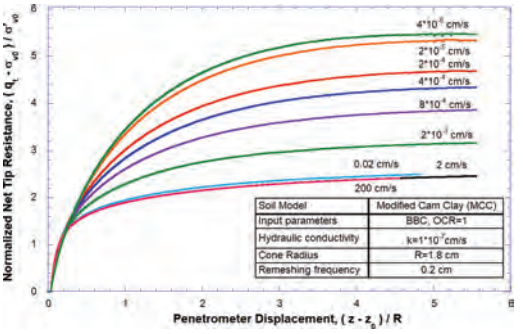

Figure 6. Effect of penetration rate on computed penetration resistance using MCC soil model.

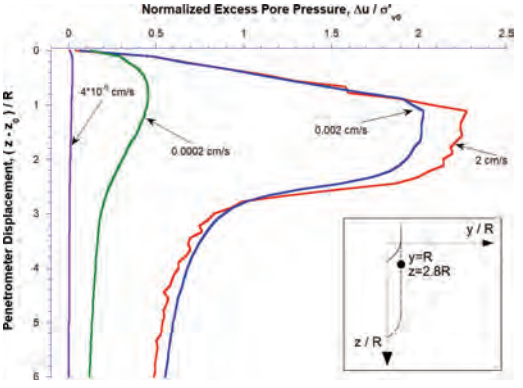

Figure 7. Effect of penetration rate on computed penetration resistance using MCC soil model.

tion rates varying from 4×10^{-6}–200cm/s. Each simulation was conducted to a minimum penetration depth, z/R = 5 with at least 50 automated remeshing steps.

The steady state penetration resistance is well defined in each of these simulations. The results show that drained penetration ($[q_t-\sigma_{v0}]/\sigma'_{v0} = 5.47$) occurs for $v \leq 2 \times 10^{-5}$cm/s; while undrained behavior is found in all case with $v \geq 0.02$cm/s ($[q_t-\sigma_{v0}]/\sigma'_{v0} = 2.45$). Partial drainage effects are observed for intermediate values of v. Figure 7 shows the computed excess pore pressures at a fixed point in the FE model (r/R = 1; z/R = 2.5). These results show that maximum excess pore pressures occur close to the base of the cone for undrained penetration, while there are no excess pore pressures in the fully drained penetration.

In order to validate the proposed FE analyses, we have attempted to replicate recent numerical simulations of piezocone tests reported by Ceccato et al. (2016) using the Material Point method (MPM). Ceccato et al. (2016) also use the MCC soil model with input parameters selected for K_0-normally consolidated kaolin. They report results corresponding to selected values of a normalized velocity, V[-] = vD/cv (after Randolph & Hope, 2004) where D is the one diameter and c_v is a constant coefficient of consolidation. In general, the stiffness of the surrounding soil will vary with the penetration induced stresses (and is therefore not constant). Ceccato et al. (2016) select a reference value (based on compression properties of NC kaolin):

$$c_v = \frac{k(1+e_0)}{\lambda \gamma_w}\sigma'_{v0} \tag{1}$$

where k is the hydraulic conductivity, e_0 and σ'_{v0} are specified initial void ratio and vertical effective stress (1.41, 50 kPa), λ is the virgin compression index (0.205) and γ_w the unit weight of water.

Figure 8 compares the FE and MPM predictions of penetration resistance for NC kaolin at selected values of V. The results show excellent agreement between the two analyses for undrained conditions (V = 501). However, the FE analyses predict higher tip resistance at lower values of the normalized velocity. For the fully drained case the FE analyses predict that a net tip resistance ($[q_t - \sigma_{v0}]/\sigma'_{v0} = 4.1$) that is 25% higher than the values reported by Ceccato et al. (2016). The source of this discrepancy requires further investigation but may be related in part to difference in the tip geometry (the MPM analyses uses a 60° conical tip, while the FE use a rounded geometry as shown in Fig. 1).

Ceccato et al. (2016) also show that there the interface friction between the cone and soil can have a large effect on penetration resistance, particularly for drained penetration. We plan to extend the current FE analyses to include effects of tip geometry and interface shear resistance.

There are a variety of laboratory tests that have been used to investigate cone resistance in nor-

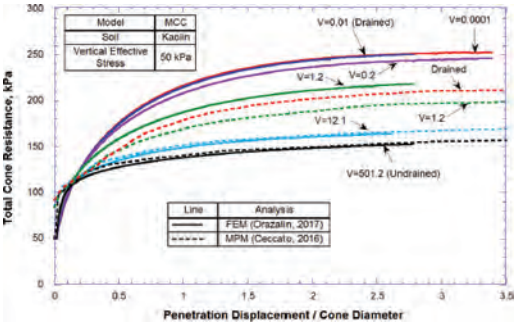

Figure 8. Comparison between proposed FE analyses and results reported using MPM method ($\mu = 0$) using MCC model for NC Kaolin.

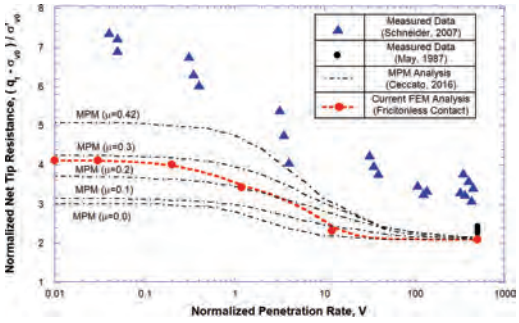

Figure 9. Comparison of computed and measured effects of partial drainage on piezocone tip resistance in kaolin.

mally consolidated kaolin including data from 1-g calibration chamber tests and centrifuge model tests. May (1987) performed a suite of tests at different penetration rates using miniature piezocones (A = 1cm^2 and 5cm^2) in 1g calibration chamber specimens with V = 480–1050 (based on lab measurements of c_v) i.e., tests in the undrained range where viscous effects are expected. Schneider et al. (2007) report results of centrifuge tests with a miniature piezocone (A = 0.079cm^2) at velocities v = 0.3 4 × 10^{-5}cm/s (V = 0.05–500, based on the reference value of c_v, Eqn. 1).

Figure 9 compares the measured net tip resistance from these experiments with the predictions from the current FE analyses and the prior MPM analyses by Ceccato et al. (2016) using a range of interface friction coefficients (μ = 0 = 0.42). In undrained conditions the FE analyses (V ≥ 50), the proposed FE analyses are in very good agreement with net tip resistance measurements in the calibration chamber, but generally underestimate the data from the centrifuge model tests. This discrepancy becomes more pronounced in slow penetration tests (drained conditions, V ≤ 0.1) where the measured tip resistance 6.9–7.4 (vs 4.1 predicted). MPM analyses of partially drained penetration predict lower tip factors than the current FE analyses (when compared with a smooth interface, m = 0). When interface friction is included the MPM model can match the measured drained tip resistance for μ 0.3.

These comparisons should be viewed as preliminary. On-going research is now focused on the role of more advanced soil model in simulating partially (and fully) drained penetration.

5 CONCLUSIONS

This paper has proposed an automated procedure for remeshing and interpolation in conjunction with a standard Lagrangian FE method to simulate large deformations caused by quasi-static piezocone penetration in soil. This methodology enables practical calculations of steady state penetration conditions with partial drainage using advanced effective stress soil models. The current paper demonstrates the accuracy of the proposed FE analysis for representing undrained penetration in clays using the MCC and MIT-E3 soil models, through comparison with prior Strain Path analyses and field measurements. Simulations of partially drained penetration (that would typically occur in transitional soils) are represented by using the MCC model to represent penetration in kaolin at a range of penetration velocities. Discrepancies from prior MPM analyses of drained penetration may be related to modeling of tip geometry and interface friction, while future studies will focus on implementations with advanced models that can represent the behavior of silts.

REFERENCES

Akl, S.A. 2010. *Wellbore instability mechanisms in clays*. PhD thesis, Massachusetts Institute of Technology, 341p.

Anura3D. 2017. *Scientific Manual for Anura3D MPM Software*, MPM Community, Ed. M. Martinelli.

Aubeny, C.P. 1992. *Rational interpretation of in-situ tests in cohesive soils*. PhD Thesis, Massachusetts Institute of Technology, 433p.

Baligh, M.M. 1985. Strain Path Method. *ASCE Journal of Geotechnical Engineering*, 111(GT9), 1131–1146.

Beuth L. 2012. *Formulation and application of a quasi-static material point method*. PhD thesis, Univ. of Stuttgart, Stuttgart, Germany.

Borouchaki, H., Laug, P. & George, P.L. 2000. Parametric surface meshing using a combined advancing-front generalized Delaunay approach. *International Journal for Numerical Methods in Engineering*, 49(1–2): 233–249.

Ceccato, F. 2015. *Study of large deformation geomechanical problems with the Material Point Method*. PhD Thesis, University of Padova.

Ceccato, F., Beuth, L., & Simonini, P. 2016. Analysis of Piezocone Penetration under Different Drainage Conditions with the Two-Phase Material Point Method. ASCE *Journal of Geotechnical and Geoenvironmental Engineering*, 142(12), 04016066-1

Hashash, Y.M.A 1992. *Analysis of deep excavations in clay*. PhD thesis, Massachusetts Institute of Technology, 344p.

Hu, Y. & Randolph, M.F. 1998. A practical numerical approach for large deformation problems in soil. *International Journal for Numerical and Analytical Methods in Geomechanics 22*(5): 327–350.

Ladd, C., Young, G.A., Kraemer, S. & Burke, D. 1999. Engineering properties of Boston Blue Clay from Special Testing Program. In *Special Geotechnical testing: Central Artery/Tunnel Project in Boston, Massachusetts, ASCE GSP 91,* 1–24.

Lu, Q., Randolph, M.F., Hu, Y. & Bugarski, I. 2004. A numerical study of cone penetration in clay. *Géotechnique 54*(4): 257–267.

May, R. 1987. *A study of the piezocone penetrometer in normally consolidated clay*, PhD Thesis, Oxford University.

McNeilan, T.W., & Bugno, W.T. 1985. Cone penetration test results in offshore California silts. Strength Testing of Marine Sediments: Laboratory and In Situ Measurements, ASTM STP 883: 55–71.

Orazalin, Z.Y. 2017. *Analysis of large deformation offshore geotechnical problems in soft clay*. PhD Thesis, MIT, 303p.

Orazalin, Z.Y., Whittle, A.J. & Olsen M.B. 2015. Three-Dimensional Analyses of Excavation Support System for the Stata Center Basement on the MIT Campus. *Journal of Geotechnical and Geoenvironmental Engineering*, 141(7).

Roscoe, K. & Burland, J.B. 1968. On the Generalized Stress-Strain Behavior of 'Wet' Clay. In *Engineering Plasticity, Cambridge University Press*, 535–609.

Schneider, J., Lehane, B.M., & Schnaid, F. 2007. Velocity effects on piezocone measurements in normally and over consolidated clays. *International Journal of Physical Modelling in Geotechnics 7*(2): 23–34.

Simulia. 2016. *Abaqus Documentation* by Dassault Systemes.

Teh, C.I., & Houlsby, G.T. 1991. An analytical study of the cone penetration test in clay. *Géotechnique*, 43(1): 17–34.

van den Berg, P. 1994. *Analysis of soil penetration*. PhD thesis, Delft University of Technology.

Whittle, A.J. & Aubeny, C.P. 1992. The effects of installation disturbance on interpretation of in-situ tests in clays. *Predictive Soil Mechanics*, Proceedings of the Wroth Memorial Symposium, Thomas Telford, London, 742–768.

Whittle, A. & Kavvadas, M. 1994. Formulation of MIT-E3 constitutive model for overconsolidated clays. *ASCE Journal of Geotechnical Engineering 120*(1), 173–198.

Whittle, A.J., DeGroot, D.J., Ladd, C.C. & Seah, T-H. 1994. Model prediction of the anisotropic behavior of Boston Blue Clay. *ASCE Journal of Geotechnical Engineering*, 120(1): 199–225.

Yi, J.T., Goh, S.H., Lee, F.H. & Randolph, M.F. 2012. A numerical study of cone penetration in fine-grained soils allowing for consolidation effects. *Géotechnique*, 62(8): 707–719.